

MORE COUNTEREXAMPLES TO THE EXTENDED COURANT PROPERTY (ECP)

PIERRE BÉRARD AND BERNARD HELFFER

ABSTRACT. The purpose of this note is to give new counterexamples to the Extended Courant Property. More precisely, we look at the equilateral rhombus, and at the hypercube, with either the Neumann or the Dirichlet boundary condition.

1. INTRODUCTION

1.1. Notation. Let $\Omega \subset \mathbb{R}^d$ be a bounded domain (Ω open and connected), with sufficiently regular boundary (say piecewise C^1 to fix the ideas).

We assume that the boundary $\Gamma = \partial\Omega$ is partitioned as

$$(1.1) \quad \Gamma = \overline{\bigsqcup_{j=1}^k \Gamma_j},$$

where the Γ_j are open subsets of $\partial\Omega$, and where \bigsqcup denotes the disjoint union.

We consider the eigenvalue problem $-\Delta u = \mu u$ in Ω , with boundary condition $\mathfrak{b}_j \in \{\mathfrak{d}, \mathfrak{n}\}$ on Γ_j , for $1 \leq j \leq k$, where \mathfrak{d} stands for *Dirichlet* boundary condition, and \mathfrak{n} for *Neumann* boundary condition. For short, we will speak of the eigenvalue problem for $(\Omega, \mathfrak{b}_1 \dots \mathfrak{b}_k)$.

Alternatively, we can consider the variational eigenvalue problem for the quadratic form $u \mapsto \int_{\Omega} |\nabla u(x)|^2 dx$ with domain $H_{\mathfrak{b}_1 \dots \mathfrak{b}_k}^1(\Omega) \subset L^2(\Omega)$, where

$$(1.2) \quad H_{\mathfrak{b}_1 \dots \mathfrak{b}_k}^1(\Omega) := \left\{ u \in H^1(\Omega) \mid u|_{\Gamma_j} = 0 \text{ whenever } \mathfrak{b}_j = \mathfrak{d} \right\}.$$

As usual, we list the eigenvalues of $(\Omega, \mathfrak{b}_1 \dots \mathfrak{b}_k)$ in nondecreasing order, with multiplicities, starting with the index 1, as

$$(1.3) \quad \mu_1(\Omega, \mathfrak{b}_1 \dots \mathfrak{b}_k) < \mu_2(\Omega, \mathfrak{b}_1 \dots \mathfrak{b}_k) \leq \mu_3(\Omega, \mathfrak{b}_1 \dots \mathfrak{b}_k) \leq \dots$$

We also use the special notation $\delta_j(\Omega)$ for the Dirichlet eigenvalues of Ω ($\mathfrak{b}_j = \mathfrak{d}$ for all j), and $\nu_j(\Omega)$ for the Neumann eigenvalues of Ω ($\mathfrak{b}_j = \mathfrak{n}$ for all j). We denote by $\text{sp}(\Omega, \mathfrak{b}_1 \dots \mathfrak{b}_k)$ the spectrum of $-\Delta$

Date: June 8, 2022 (berard-helffer-ecp-newex-180227.tex).

2010 Mathematics Subject Classification. 35P99, 35Q99, 58J50.

Key words and phrases. Eigenfunction, Nodal domain, Courant nodal domain theorem.

for $(\Omega, \mathbf{b}_1 \cdots \mathbf{b}_k)$. To make notation lighter, we skip mentioning Ω , or the boundary condition $\mathbf{b}_1 \cdots \mathbf{b}_k$, whenever the context is clear.

We denote by $\mathcal{E}(\mu_m(\Omega, \mathbf{b}_1 \cdots \mathbf{b}_k))$ the eigenspace of $-\Delta$ associated with the eigenvalue $\mu_m(\Omega, \mathbf{b}_1 \cdots \mathbf{b}_k)$, and we use the notation $\mathcal{E}(\mu_m)$ when the context (domain, boundary condition) is clear. We denote by $\text{mult}(\mu)$ the multiplicity of the eigenvalue μ , i.e., the dimension of $\mathcal{E}(\mu)$, with the convention that $\text{mult}(\mu) = 0$ if μ is not an eigenvalue.

We denote by $\mathcal{Z}(u)$ the *nodal set* of a continuous function u ,

$$(1.4) \quad \mathcal{Z}(u) = \overline{\{x \in \Omega \mid u(x) = 0\}},$$

and by $\beta_0(u)$ the number of *nodal domains* of u ,

$$(1.5) \quad \beta_0(u) = \text{number of connected components of } \Omega \setminus \mathcal{Z}(u).$$

Given an eigenvalue μ of $(\Omega, \mathbf{b}_1 \cdots \mathbf{b}_k)$, we introduce the index

$$(1.6) \quad \kappa(\mu) := \min\{m \mid \mu = \mu_m(\Omega, \mathbf{b}_1 \cdots \mathbf{b}_k)\}.$$

1.2. The extended Courant Property. A celebrated theorem of Richard Courant (1923, see [4, § VI.6]) states that

$$(1.7) \quad \beta_0(u) \leq \kappa(\mu_m) \leq m \text{ for any } u \in \mathcal{E}(\mu_m(\Omega, \mathbf{b}_1 \cdots \mathbf{b}_k)).$$

A footnote in [4, p. 454] states that the same inequality actually holds for any linear combination of eigenfunctions associated with eigenvalues less than or equal to μ_m ,

$$(1.8) \quad \beta_0(v) \leq \kappa(\mu_m) \leq m \text{ for any } v = \sum_{\mu_j \leq \mu_m} u_{\mu_j}, \quad u_{\mu_j} \in \mathcal{E}(\mu_j),$$

and refers wrongly to the 1932 PhD Thesis of Horst Herrmann [6].

We call inequality (1.8) the *Extended Courant Property* for the domain Ω , and refer to it as the $\text{ECP}(\Omega)$, or as the $\text{ECP}(\Omega, \mathbf{b})$ to insist on the boundary condition \mathbf{b} . It turns out that, for $d \geq 2$, there exist domains Ω for which the $\text{ECP}(\Omega)$ is false. We refer to [3] for references, historical remarks and some counterexamples.

1.3. Purpose and organization of this note. The purpose of this note is to give new counterexamples to the ECP . In Section 2, we consider the case of the equilateral rhombus. We give a counterexample to the ECP for the Neumann boundary condition. Numerical simulations indicate that there are counterexamples for the Dirichlet boundary condition as well. In Section 3, we consider the case of the hypercube with either Dirichlet or Neumann boundary conditions.

2. THE EQUILATERAL RHOMBUS

2.1. Preparation. Let $\mathcal{R}h_e$ be the equilateral rhombus with sides of length 1, and vertices $(0, 0)$, $(1, 0)$, $(\frac{3}{2}, \frac{\sqrt{3}}{2})$ and $(\frac{1}{2}, \frac{\sqrt{3}}{2})$. Call D and M its diagonals (resp. the longer one and the shorter one), see Figure 2.1.

Call \mathcal{T}_e the equilateral triangle with vertices $(0, 0)$, $(1, 0)$, and $(\frac{1}{2}, \frac{\sqrt{3}}{2})$. Call \mathcal{T}_h the hemiequilateral triangle with vertices $(0, 0)$, $(\frac{\sqrt{3}}{2}, 0)$ and $(\frac{\sqrt{3}}{2}, \frac{1}{2})$. The diagonal M divides the rhombus into two equilateral triangles $\mathcal{T}_{e,1}$ and $\mathcal{T}_{e,2}$, isometric to \mathcal{T}_e . The diagonals D and M divide the rhombus into four hemiequilateral triangles $\mathcal{T}_{h,j}$, $1 \leq j \leq 4$, isometric to \mathcal{T}_h , see Figure 2.2. In the sequel, we also use the generic notation \mathcal{T}_e (resp. \mathcal{T}_h) for any of the equilateral triangles (resp. hemiequilateral triangles) into which the rhombus decomposes.

We also denote by D and M the mirror symmetries with respect to the lines supporting the diagonals of the rhombus, and by D^* and M^* the action of these symmetries on functions, for example $D^*f = f \circ D$.

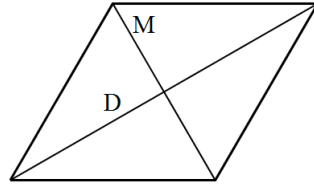


FIGURE 2.1. The equilateral rhombus $\mathcal{R}h_e$, and its diagonals

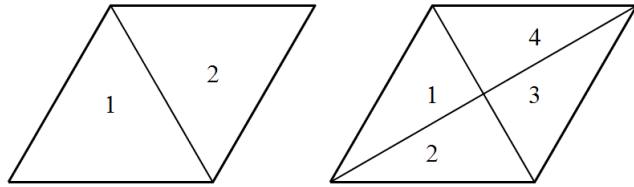


FIGURE 2.2. Decomposition of the equilateral rhombus $\mathcal{R}h_e$

The symmetries D and M act by isometries on the rhombus, and they commute. The eigenspaces of $-\Delta$ for $(\mathcal{R}h_e, \mathfrak{b})$, with $\mathfrak{b} \in \{\mathfrak{d}, \mathfrak{n}\}$, decompose into summands corresponding to the action of these symmetries. The eigenfunctions in each summand correspond to eigenfunctions of $-\Delta$ for the equilateral or hemiequilateral triangles into which the rhombus decomposes, with the boundary condition \mathfrak{b} on the sides supported

by $\partial\mathcal{R}h_e$, and with mixed boundary conditions, either Dirichlet or Neumann, on the sides supported by the diagonals.

To be more explicit, we need naming the eigenvalues according to Subsection 1.1. For this purpose, we partition the boundaries of \mathcal{T}_e and \mathcal{T}_h into their three sides. For \mathcal{T}_h , we number the sides 1, 2, 3, in decreasing order of length, see Figure 2.3. For example, $\mu_i(\mathcal{T}_h, \mathbf{n}\mathbf{d}\mathbf{n})$ denotes the i -th eigenvalue of $-\Delta$ in \mathcal{T}_h with Neumann boundary condition on the longest (1) and shortest (3) sides, and Dirichlet boundary condition on the other side (2).

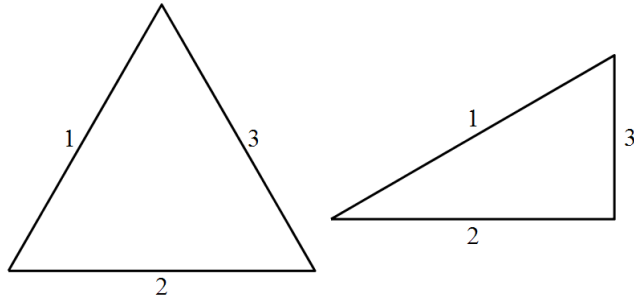


FIGURE 2.3. Labelling the sides of \mathcal{T}_e and \mathcal{T}_h

More precisely, we decompose the space $L^2(\mathcal{R}h_e)$ into orthogonal components,

$$(2.1) \quad L^2(\mathcal{R}h_e) = \mathcal{S}_{+,+} \bigoplus \mathcal{S}_{+,-} \bigoplus \mathcal{S}_{-,+} \bigoplus \mathcal{S}_{-,-},$$

where

$$(2.2) \quad \mathcal{S}_{\sigma,\tau} := \left\{ \phi \in L^2(\mathcal{R}h_e) \mid D^* \phi = \sigma \phi \text{ and } M^* \phi = \tau \phi \right\},$$

for $\sigma, \tau \in \{+, -\}$.

Since the isometries D^* and M^* commute with Δ , this orthogonal decomposition descends to each eigenspace of $-\Delta$ for $(\mathcal{R}h_e, \mathbf{b})$, with the boundary condition $\mathbf{b} \in \{\mathbf{d}, \mathbf{n}\}$ on the boundary $\partial\mathcal{R}h_e$.

2.2. A reflection principle. In this subsection, we explain an elementary but useful ‘‘reflection principle’’ which we will use repeatedly in the sequel.

Consider the decomposition $\mathcal{R}h_e = \mathcal{T}_{e,1} \sqcup \mathcal{T}_{e,2}$. Note that $M(\mathcal{T}_{e,1}) = \mathcal{T}_{e,2}$. Choose a boundary condition $\mathbf{a} \in \{\mathbf{d}, \mathbf{n}\}$ on $\partial\mathcal{R}h_e$. Given an eigenvalue λ of $-\Delta$ for $(\mathcal{R}h_e, \mathbf{a})$, and $\sigma \in \{+, -\}$, consider the subspace $\mathcal{E}(\lambda) \cap \mathcal{S}_{M,\sigma}$ of eigenfunctions $\phi \in \mathcal{E}(\lambda)$ such that $M^* \phi = \sigma \phi$.

If $0 \neq \phi \in \mathcal{E}(\lambda) \cap \mathcal{S}_{M,\sigma}$, then $\phi|_{\mathcal{T}_{e,1}}$ is an eigenfunction of $-\Delta$ for $(\mathcal{T}_{e,1}, \mathbf{a}\mathbf{a}\mathbf{b})$, with $\mathbf{b} = \mathbf{n}$ if $\sigma = +$, and $\mathbf{b} = \mathbf{d}$ if $\sigma = -$, associated with the same eigenvalue λ .

Conversely, let ψ be an eigenfunction of $(\mathcal{T}_{e,1}, \mathfrak{aab})$, with eigenvalue $\mu_m(\mathcal{T}_{e,1}, \mathfrak{aab})$, for some $m \geq 1$. Define the function $\check{\psi}$ on $\mathcal{R}h_e$ such that $\check{\psi}|_{\mathcal{T}_{e,1}} = \psi$ and $\check{\psi}|_{\mathcal{T}_{e,2}} = \sigma \psi \circ M$. This means that $\check{\psi}$ is obtained by extending ψ across M to $\mathcal{T}_{e,2}$ by symmetry, in such a way that $M^* \check{\psi} = \sigma \check{\psi}$. It is easy to see that the function $\check{\psi}$ is an eigenfunction of $-\Delta$ for $(\mathcal{R}h_e, \mathfrak{n})$ (in particular it is smooth in a neighborhood of M), with eigenvalue $\mu_m(\mathcal{T}_{e,1}, \mathfrak{aab})$, so that $\check{\psi} \in \mathcal{E}(\mu_m) \cap \mathcal{S}_{M,\sigma}$.

The above considerations prove the first two assertions in the following proposition. The proof of the third and fourth assertions is similar, using the symmetries D and M , and the decomposition of $\mathcal{R}h_e$ into the triangles $\mathcal{T}_{h,j}$, $1 \leq j \leq 4$.

Proposition 2.1 (Reflection principle). *For any $\mathfrak{a} \in \{\mathfrak{d}, \mathfrak{n}\}$ and any $\lambda \in \text{sp}(\mathcal{R}h_e, \mathfrak{a})$,*

- (i) $\mathcal{E}(\lambda, (\mathcal{R}h_e, \mathfrak{a})) \cap \mathcal{S}_{M,+} \neq \{0\}$ if and only if $\lambda \in \text{sp}(\mathcal{T}_e, \mathfrak{aan})$, and the map $\phi \mapsto \phi|_{\mathcal{T}_{e,1}}$ is a bijection from $\mathcal{E}(\lambda, (\mathcal{R}h_e, \mathfrak{a})) \cap \mathcal{S}_{M,+}$ onto $\mathcal{E}(\lambda, (\mathcal{T}_e, \mathfrak{aan}))$;
- (ii) $\mathcal{E}(\lambda, (\mathcal{R}h_e, \mathfrak{a})) \cap \mathcal{S}_{M,-} \neq \{0\}$ if and only if $\lambda \in \text{sp}(\mathcal{T}_e, \mathfrak{aad})$, and the map $\phi \mapsto \phi|_{\mathcal{T}_{e,1}}$ is a bijection from $\mathcal{E}(\lambda, (\mathcal{R}h_e, \mathfrak{a})) \cap \mathcal{S}_{M,-}$ onto $\mathcal{E}(\lambda, (\mathcal{T}_e, \mathfrak{aad}))$.

More generally, for any $\lambda \in \text{sp}(\mathcal{R}h_e, \mathfrak{a})$, and any $\mathfrak{b}, \mathfrak{c} \in \{\mathfrak{d}, \mathfrak{n}\}$,

- (iii) $\mathcal{E}(\lambda, (\mathcal{R}h_e, \mathfrak{a})) \cap \mathcal{S}_{\epsilon(\mathfrak{b}), \epsilon(\mathfrak{c})} \neq \{0\}$ if and only if $\lambda \in \text{sp}(\mathcal{T}_h, \mathfrak{abc})$, and the map $\phi \mapsto \phi|_{\mathcal{T}_{h,1}}$ is a bijection from $\mathcal{E}(\lambda, (\mathcal{R}h_e, \mathfrak{a})) \cap \mathcal{S}_{\epsilon(\mathfrak{b}), \epsilon(\mathfrak{c})}$ onto $\mathcal{E}(\lambda, (\mathcal{T}_h, \mathfrak{abc}))$. Here $\epsilon(\mathfrak{n}) = +$ and $\epsilon(\mathfrak{d}) = -$.

Furthermore, the multiplicity of the number λ as eigenvalue of $(\mathcal{R}h_e, \mathfrak{a})$ is the sum, over $\mathfrak{b}, \mathfrak{c} \in \{\mathfrak{d}, \mathfrak{n}\}$, of the multiplicities of λ as eigenvalue of $(\mathcal{T}_h, \mathfrak{abc})$ (with the convention that the multiplicity is zero if λ is not an eigenvalue).

2.3. Some useful results. In this subsection, we recall some known results for the reader's convenience.

2.3.1. *Eigenvalue inequalities.* The following proposition is a particular case of a result of V. Lotoreichik and J. Rohleder [7, Proposition 2.3].

Proposition 2.2. *For the triangle \mathcal{T}_h , and for any $i \geq 1$, we have the inequalities,*

$$(2.3) \quad \begin{cases} \mu_i(\mathcal{T}_h, \mathfrak{nnn}) < \mu_i(\mathcal{T}_h, \mathfrak{nnd}) < \mu_i(\mathcal{T}_h, \mathfrak{ndd}), \\ \mu_i(\mathcal{T}_h, \mathfrak{nnn}) < \mu_i(\mathcal{T}_h, \mathfrak{nnd}) < \mu_i(\mathcal{T}_h, \mathfrak{ndd}), \end{cases}$$

and

$$(2.4) \quad \begin{cases} \mu_i(\mathcal{T}_h, \mathfrak{dnn}) < \mu_i(\mathcal{T}_h, \mathfrak{ddn}) < \mu_i(\mathcal{T}_h, \mathfrak{ddd}), \\ \mu_i(\mathcal{T}_h, \mathfrak{dnn}) < \mu_i(\mathcal{T}_h, \mathfrak{dnd}) < \mu_i(\mathcal{T}_h, \mathfrak{ddd}). \end{cases}$$

The following inequalities are due to B. Siudeja [8, Theorem 1.1].

Proposition 2.3. *Let $\mathcal{T}_r(\alpha)$ be a right triangle with smallest angle α , such that $\frac{\pi}{6} \leq \alpha \leq \frac{\pi}{4}$, and sides numbered in non-increasing order. Its eigenvalues satisfy the following inequalities.*

- *If $\frac{\pi}{6} < \alpha < \frac{\pi}{4}$,*

$$0 = \nu_1 < \mu_1(\mathbf{nnd}) < \mu_1(\mathbf{n\bar{d}n}) < \nu_2 < \mu_1(\mathbf{dnn}) \cdots \\ \cdots < \mu_1(\mathbf{n\bar{d}\bar{d}}) < \mu_1(\mathbf{d\bar{n}d}) < \mu_1(\mathbf{d\bar{d}n}) < \delta_1.$$

- *If $\frac{\pi}{6} = \alpha$,*

$$0 = \nu_1 < \mu_1(\mathbf{nnd}) < \mu_1(\mathbf{n\bar{d}n}) = \nu_2 < \mu_1(\mathbf{dnn}) \cdots \\ \cdots < \mu_1(\mathbf{n\bar{d}\bar{d}}) < \mu_1(\mathbf{d\bar{n}d}) < \mu_1(\mathbf{d\bar{d}n}) < \delta_1.$$

- *If $\alpha = \frac{\pi}{4}$,*

$$0 = \nu_1 < \mu_1(\mathbf{nnd}) < \mu_1(\mathbf{n\bar{d}n}) < \nu_2 = \mu_1(\mathbf{dnn}) \cdots \\ \cdots < \mu_1(\mathbf{n\bar{d}\bar{d}}) < \mu_1(\mathbf{d\bar{n}d}) = \mu_1(\mathbf{d\bar{d}n}) < \delta_1.$$

Remark 2.4. *We do not know if there exist, for $i \geq 2$, any general inequalities between the eigenvalues $\mu_i(\mathcal{T}_h, \mathbf{n\bar{d}n})$ and $\mu_i(\mathcal{T}_h, \mathbf{nnd})$ in (2.3), or between the eigenvalues $\mu_i(\mathcal{T}_h, \mathbf{d\bar{d}n})$ and $\mu_i(\mathcal{T}_h, \mathbf{d\bar{n}d})$ in (2.4).*

2.3.2. Eigenvalues of some mixed boundary value problems for \mathcal{T}_h . For later reference, we also describe the eigenvalues and eigenfunctions of four mixed eigenvalue problems for \mathcal{T}_h . This description follows easily for example from [3, Appendix A] and [2].

The eigenvalues of the equilateral triangle \mathcal{T}_e , with either the Dirichlet or the Neumann boundary condition on $\partial\mathcal{T}_e$, are the numbers

$$(2.5) \quad \hat{\lambda}(m, n) = \frac{16\pi^2}{9} (m^2 + mn + n^2),$$

with $(m, n) \in \mathbb{N} \times \mathbb{N}$ for the Neumann boundary condition, and $(m, n) \in \mathbb{N}^\bullet \times \mathbb{N}^\bullet$ for the Dirichlet boundary condition (here $\mathbb{N}^\bullet = \mathbb{N} \setminus \{0\}$). The multiplicities are given by,

$$(2.6) \quad \text{mult}(\hat{\lambda}_0) = \# \left\{ (m, n) \in \mathcal{L} \mid \hat{\lambda}(m, n) = \hat{\lambda}_0 \right\},$$

with $\mathcal{L} = \mathbb{N} \times \mathbb{N}$ for the Neumann boundary condition, and $\mathcal{L} = \mathbb{N}^\bullet \times \mathbb{N}^\bullet$ for the Dirichlet boundary condition.

One can associate one or two real eigenfunctions with such a pair (m, n) . When $m = n$, there is only one associated eigenfunction, and it is D -invariant. When $m \neq n$, there are two associated eigenfunctions, one symmetric with respect to D , the other one anti-symmetric. As a consequence, one can explicitly describe the eigenvalues and eigenfunctions of the four eigenvalue problems $(\mathcal{T}_h, \mathbf{n\bar{n}n})$, $(\mathcal{T}_h, \mathbf{n\bar{d}n})$ (they arise from the Neumann problem for \mathcal{T}_e), and $(\mathcal{T}_h, \mathbf{d\bar{n}d})$, $(\mathcal{T}_h, \mathbf{d\bar{d}n})$ (they arise from the Dirichlet problem for \mathcal{T}_e).

The resulting eigenvalues are given in Table 2.1.

Eigenvalue problem	Eigenvalues
$(\mathcal{T}_h, \mathbf{nnn})$	$\hat{\lambda}(m, n)$, for $0 \leq m \leq n$
$(\mathcal{T}_h, \mathbf{n}\partial\mathbf{n})$	$\hat{\lambda}(m, n)$, for $0 \leq m < n$
$(\mathcal{T}_h, \mathbf{d}\partial\mathbf{d})$	$\hat{\lambda}(m, n)$, for $1 \leq m \leq n$
$(\mathcal{T}_h, \mathbf{d}\mathbf{d}\mathbf{d})$	$\hat{\lambda}(m, n)$, for $1 \leq m < n$

TABLE 2.1. Four mixed eigenvalue problems for \mathcal{T}_h

Remark 2.5. *As far as we know, there are no such explicit formulas for the eigenvalues of the other mixed boundary value problems for \mathcal{T}_h .*

The following tables, display the first few eigenvalues, the corresponding pairs of integers, and the corresponding indexed eigenvalues for the given mixed boundary value problems for \mathcal{T}_h .

Eigenvalue	Pairs	$(\mathcal{T}_h, \mathbf{nnn})$	$(\mathcal{T}_h, \mathbf{n}\partial\mathbf{n})$
0	(0, 0)	μ_1	
$\frac{16\pi^2}{9}$	(0, 1), (1, 0)	μ_2	μ_1
$3 \times \frac{16\pi^2}{9}$	(1, 1)	μ_3	
$4 \times \frac{16\pi^2}{9}$	(0, 2), (2, 0)	μ_4	μ_2
$7 \times \frac{16\pi^2}{9}$	(1, 2), (2, 1)	μ_5	μ_3
$9 \times \frac{16\pi^2}{9}$	(0, 3), (3, 0)	μ_6	μ_4

TABLE 2.2. First eigenvalues for $(\mathcal{T}_h, \mathbf{nnn})$ and $(\mathcal{T}_h, \mathbf{n}\partial\mathbf{n})$

Eigenvalue	Pairs	$(\mathcal{T}_h, \mathbf{d}\partial\mathbf{d})$	$(\mathcal{T}_h, \mathbf{d}\mathbf{d}\mathbf{d})$
$3 \times \frac{16\pi^2}{9}$	(1, 1)	μ_1	
$7 \times \frac{16\pi^2}{9}$	(1, 2), (2, 1)	μ_2	μ_1
$12 \times \frac{16\pi^2}{9}$	(2, 2)	μ_3	
$13 \times \frac{16\pi^2}{9}$	(1, 3), (3, 1)	μ_4	μ_2
$19 \times \frac{16\pi^2}{9}$	(2, 3), (3, 2)	μ_5	μ_3
$21 \times \frac{16\pi^2}{9}$	(1, 4), (4, 1)	μ_6	μ_4

TABLE 2.3. First eigenvalues for $(\mathcal{T}_h, \mathbf{d}\partial\mathbf{d})$ and $(\mathcal{T}_h, \mathbf{d}\mathbf{d}\mathbf{d})$

Remark 2.6. *For later reference, we point out that all the eigenvalues which appear in Tables 2.2 and 2.3 are simple.*

2.4. Rhombus with Neumann boundary condition. In this subsection, we take the Neumann boundary condition on the boundary $\partial\mathcal{R}h_e$ of the equilateral rhombus.

2.4.1. *The first Neumann eigenvalues of $\mathcal{R}h_e$.*

Proposition 2.7. *For $(\mathcal{R}h_e, \mathfrak{n})$, we have*

$$(2.7) \quad 0 = \nu_1 < \nu_2 < \nu_3 = \nu_4 < \nu_5 \leq \cdots$$

More precisely,

(i) The second eigenvalue ν_2 is simple and satisfies

$$(2.8) \quad \nu_2 = \mu_1(\mathcal{T}_e, \mathfrak{nnd}) = \mu_1(\mathcal{T}_h, \mathfrak{nnd}) .$$

If $\psi_2 \in \mathcal{E}(\nu_2)$, then it is invariant under the symmetry D , anti-invariant under the symmetry M , and $\mathcal{Z}(\psi_2) = M$.

Furthermore, $\psi_2|\mathcal{T}_h$ is a first eigenfunction of $(\mathcal{T}_h, \mathfrak{nnd})$, and $\psi_2|\mathcal{T}_e$ is a first eigenfunction of $(\mathcal{T}_e, \mathfrak{nnd})$.

(ii) For the eigenspace $\mathcal{E}(\nu_3)$ we have

$$(2.9) \quad \begin{cases} \dim(\mathcal{E}(\nu_3) \cap \mathcal{S}_{+,+}) = \dim(\mathcal{E}(\nu_3) \cap \mathcal{S}_{-,+}) = 1, \\ \mathcal{E}(\nu_3) \cap \mathcal{S}_{-,-} = \mathcal{E}(\nu_3) \cap \mathcal{S}_{+,-} = \{0\} . \end{cases}$$

In particular, the eigenspace $\mathcal{E}(\nu_3)$ is spanned by two linearly independent functions ψ_3 and ψ_4 which are M invariant, and whose restrictions to \mathcal{T}_e generate the eigenspace $\mathcal{E}(\nu_2(\mathcal{T}_e))$.

Proof. According to the Reflection principle, Proposition 2.1, the first six eigenvalues of $(\mathcal{R}h_e, \mathfrak{n})$ belong to the set

$$(2.10) \quad \{\mu_i(\mathcal{T}_h, \mathfrak{nab}) \text{ for } 1 \leq i \leq 6 \text{ and } \mathfrak{a}, \mathfrak{b} \in \{\mathfrak{d}, \mathfrak{n}\}\} .$$

Among these numbers, the eigenvalues of $(\mathcal{T}_h, \mathfrak{n}nn)$ and $(\mathcal{T}_h, \mathfrak{n}dn)$ are known explicitly, and they are simple, see Tables 2.2.

Although the eigenvalues and eigenfunctions of $(\mathcal{T}_h, \mathfrak{nnd})$ and $(\mathcal{T}_h, \mathfrak{dnn})$ are, as far as we know, not explicitly known, they satisfy some inequalities: the obvious inequalities $\mu_1 < \mu_2 \leq \cdots$, and the inequalities provided by Proposition 2.2 (see [7]), and Proposition 2.3 (see [8]).

Table 2.4 summarizes what we know about the eigenvalues which appear in (2.10). In blue the known values, in red the known inequalities. The gray cells contain the eigenvalues, listed with multiplicities, for which we have no a priori information, except the trivial inequalities (black inequality signs).

Remark 2.8. *Note that we only display the first four eigenvalues in each line, because this turns out to be sufficient.*

Remark 2.9. *The reason why there are white empty cells in the 5th row is explained in Remark 2.4.*

Upon inspection of Table 2.4, we conclude that the Neumann eigenvalues of $\mathcal{R}h_e$ satisfy the following inequalities

$$(2.11) \quad 0 = \nu_1 < \nu_2 < \nu_3 = \nu_4 < \nu_5 \leq \nu_6 \leq \cdots ,$$

(σ, τ)	$(\mathcal{T}_h, \mathbf{nab})$	μ_1		μ_2		μ_3		μ_4
$(+, +)$	$(\mathcal{T}_h, \mathbf{nnn})$	0	<	$\frac{16\pi^2}{9}$	<	$3 \frac{16\pi^2}{9}$	<	$4 \frac{16\pi^2}{9}$
		Λ		Λ		Λ		Λ
$(+, -)$	$(\mathcal{T}_h, \mathbf{nnd})$		<		\leq		\leq	
		Λ						
$(-, +)$	$(\mathcal{T}_h, \mathbf{ndn})$	$\frac{16\pi^2}{9}$	<	$4 \frac{16\pi^2}{9}$	<	$7 \frac{16\pi^2}{9}$	<	$9 \frac{16\pi^2}{9}$
		Λ		Λ		Λ		Λ
$(-, -)$	$(\mathcal{T}_h, \mathbf{nnd})$		<		\leq		\leq	

TABLE 2.4. $\mathcal{R}h_e$, Neumann boundary condition

with

$$\nu_2 = \mu_1(\mathcal{T}_h, \mathbf{nnd}), \nu_3 = \mu_1(\mathcal{T}_h, \mathbf{ndn}) = \mu_2(\mathcal{T}_h, \mathbf{nnn}).$$

We can a priori not draw any conclusion on ν_5, ν_6, \dots

Table 2.4 actually provides further information,

$$(2.12) \quad \begin{cases} \dim \mathcal{E}(\nu_1) \cap \mathcal{S}_{+,+} = 1, \\ \mathcal{E}(\nu_1) \cap \mathcal{S}_{\sigma,\tau} = \{0\} \text{ if } (\sigma, \tau) \neq (+, +), \\ \dim \mathcal{E}(\nu_2) \cap \mathcal{S}_{+,-} = 1, \\ \mathcal{E}(\nu_2) \cap \mathcal{S}_{\sigma,\tau} = \{0\} \text{ if } (\sigma, \tau) \neq (+, -), \\ \dim \mathcal{E}(\nu_3) \cap \mathcal{S}_{+,+} = \dim \mathcal{E}(\nu_3) \cap \mathcal{S}_{+,-} = 1, \\ \dim \mathcal{E}(\nu_3) \cap \mathcal{S}_{\sigma,\tau} = \{0\} \text{ if } (\sigma, \tau) = (-, +) \text{ or } (-, -). \end{cases}$$

The equality $\nu_3 = \nu_4$ comes from the fact that the second Neumann eigenvalue of the equilateral triangle has multiplicity 2, with an eigen-space generated by one eigenfunction which is symmetric with respect to a side bisector, and another one which is anti-symmetric.

Note: For the reader's information, Table 2.5, displays numerical values for the eigenvalues: in the gray cells, the numerical values computed with MATLAB; in the other cells, the approximate values of the known eigenvalues.

(σ, τ)	$(\mathcal{T}_h, \mathbf{nab})$	μ_1		μ_2		μ_3		μ_4
$(+, +)$	$(\mathcal{T}_h, \mathbf{n}nn)$	0	<	17.55	<	52.64	<	70.18
		Λ		Λ		Λ		Λ
$(+, -)$	$(\mathcal{T}_h, \mathbf{n}nd)$	7.16	<	37.49	≤	90.06	≤	120.87
		Λ						
$(-, +)$	$(\mathcal{T}_h, \mathbf{n}dn)$	17.55	<	70.18	<	122.82	<	157.91
		Λ		Λ		Λ		Λ
$(-, -)$	$(\mathcal{T}_h, \mathbf{n}dd)$	47.63	<	110.36	≤	189.52	≤	224.68

TABLE 2.5. $\mathcal{R}h_e$, Neumann boundary condition

The proof of Proposition 2.7 is complete. \square

Remark 2.10. One can also deduce Proposition 2.7 from the proof of Corollary 1.3 in [8] which establishes that the first four Neumann eigenvalues of a rhombus $\mathcal{R}h(\alpha)$ with smallest angle $2\alpha > \frac{\pi}{3}$ are simple, and describes the nodal patterns of the corresponding eigenvalues. When $2\alpha = \frac{\pi}{3}$ the eigenvalues ν_3 and ν_4 become equal, see also Remarks 4.1 and 4.2 in [8].

2.4.2. *The Extended Courant Property for $\mathcal{R}h_e$.* As a corollary of Proposition 2.7, we obtain,

Proposition 2.11. *The equilateral rhombus with Neumann boundary condition provides a counterexample to the ECP. More precisely, there is a linear combination of eigenfunctions in $\mathcal{E}(\nu_1) \oplus \mathcal{E}(\nu_3)$ with four nodal domains.*

Proof. Proposition 2.7, Assertion (ii) tells us that $\mathcal{E}(\nu_3)$ contains an eigenfunction which comes from the second Neumann eigenfunction of $\mathcal{T}_{e,1} = \mathcal{T}_e$ which is symmetric with respect to D . It then suffices to apply the same arguments as in [3, Section 6.1]. A second Neumann eigenfunction for \mathcal{T}_e is given by

$$(2.13) \quad \phi_2^N(x, y) = 2 \cos\left(\frac{2\pi x}{3}\right) \left(\cos\left(\frac{2\pi x}{3}\right) + \cos\left(\frac{2\pi y}{\sqrt{3}}\right) \right) - 1.$$

Extend this function, by symmetry with respect to M , to a function ϕ_2 in $\mathcal{R}h_e$. The linear combination $\phi_2 + 1$ vanishes on the line segments $\{x = \frac{3}{4}\} \cap \mathcal{R}h_e$ and $\{x + \sqrt{3}y = \frac{3}{2}\} \cap \mathcal{R}h_e$, so that it has four nodal domains, see Figure 2.4, contradicting Courant's theorem. \square

Figure 2.5 displays the MATLAB rendering of the variation of the number of nodal domains (the eigenfunction produced by MATLAB is proportional to ϕ_2 , not equal, so that the bifurcation value is not 1 as in the proof of Proposition 2.11).

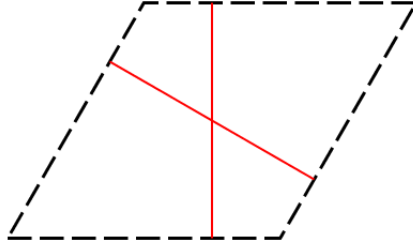


FIGURE 2.4. Nodal pattern of some linear combination in $\mathcal{E}(\nu_1) \oplus \mathcal{E}(\nu_3)$, with four nodal domains

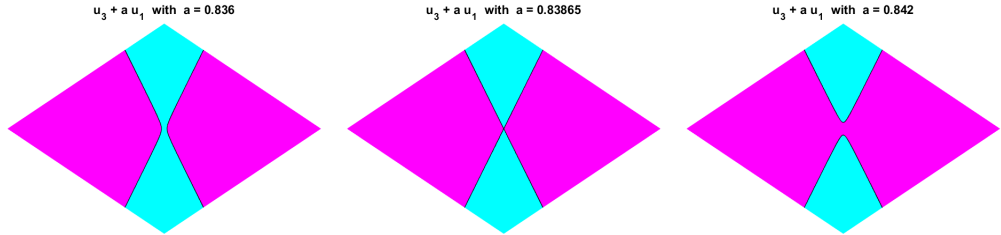
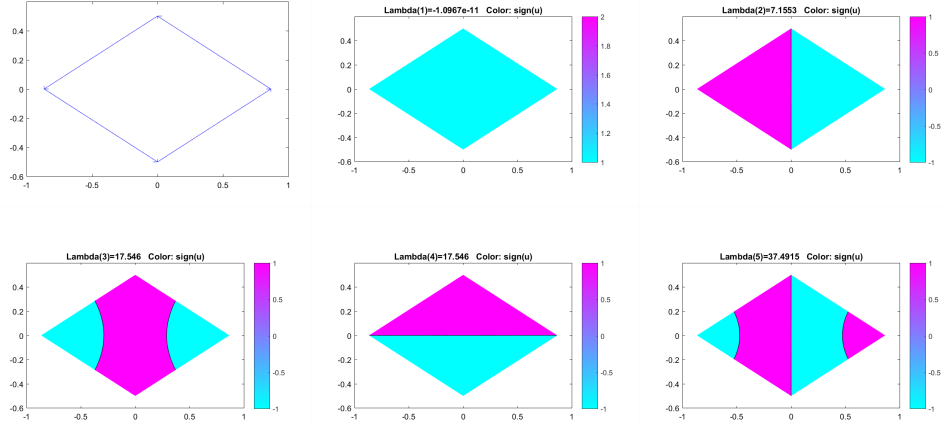
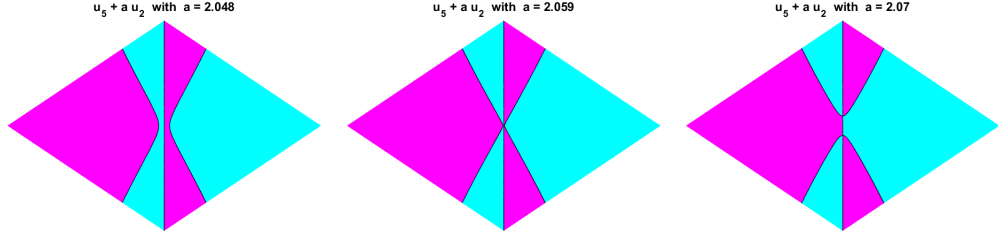


FIGURE 2.5. Nodal patterns of linear combinations in $\mathcal{E}(\nu_1) \oplus \mathcal{E}(\nu_3)$ around the bifurcation

2.4.3. *A numerical result for $\mathcal{R}h_e$ with Neumann boundary condition.* Numerical computations for the first Neumann eigenvalues of the equilateral rhombus give,

$$(2.14) \quad 0 = \nu_1 < \nu_2 < \nu_3 = \nu_4 < \nu_5 < \nu_6 < \nu_7 \dots ,$$

with the first five nodal patterns shown in Figure 2.6. Numerical computations of the eigenfunctions show that there are linear combinations in $\mathcal{E}(\nu_2) \oplus \mathcal{E}(\nu_5)$ with six nodal domains, thus providing another (numerical) counterexample to the ECP($\mathcal{R}h_e, \mathfrak{n}$), see Figure 2.7. This counterexample can also be interpreted as a counterexample to the ECP for the equilateral triangle with mixed boundary conditions, Neumann on two sides, and Dirichlet on the third side.

FIGURE 2.6. Rhombus $\mathcal{R}h_e$, Neumann boundary conditionFIGURE 2.7. Nodal patterns of some linear combinations in $\mathcal{E}(\nu_2) \oplus \mathcal{E}(\nu_5)$

2.5. Rhombus with Dirichlet boundary condition. We now describe the first three eigenvalues of $(\mathcal{R}h_e, \mathfrak{d})$, although this does not produce any counterexample to the ECP($\mathcal{R}h_e, \mathfrak{d}$).

Proposition 2.12. *The first three eigenvalues of $(\mathcal{R}h_e, \mathfrak{d})$ satisfy*

$$(2.15) \quad \delta_1 < \delta_2 < \delta_3 \leq \delta_4 \dots$$

More precisely,

- (i) $\delta_1(\mathcal{R}h_e) = \mu_1(\mathcal{T}_e, \mathfrak{d}\mathfrak{d}\mathfrak{n}) = \mu_1(\mathcal{T}_h, \mathfrak{d}\mathfrak{n}\mathfrak{n})$ is simple, with eigenfunction in $\mathcal{S}_{+,+}$.
- (ii) $\delta_2(\mathcal{R}h_e) = \delta_1(\mathcal{T}_e)$ is simple, with eigenfunction in $\mathcal{S}_{+,-}$.
- (iii) We have $\delta_3(\mathcal{R}h_e) = \delta_1(\mathcal{T}_h, \mathfrak{d}\mathfrak{d}\mathfrak{n})$, with a corresponding eigenfunction in $\mathcal{S}_{-,+}$.

Proof. Assertion (i) is clear.

According to the Reflection principle, Proposition 2.1, the first four eigenvalues of $(\mathcal{R}h_e, \mathfrak{d})$ belong to the set

$$(2.16) \quad \{\mu_i(\mathcal{T}_h, \mathfrak{d}\mathfrak{a}\mathfrak{b}) \text{ for } 1 \leq i \leq 4 \text{ and } \mathfrak{a}, \mathfrak{b} \in \{\mathfrak{d}, \mathfrak{n}\}\} .$$

Among these numbers, the eigenvalues of $(\mathcal{T}_h, \mathfrak{d}\mathfrak{n}\mathfrak{d})$ and $(\mathcal{T}_h, \mathfrak{d}\mathfrak{d}\mathfrak{d})$ are known explicitly, they are simple eigenvalues, see Tables 2.3.

As in Section 2.4, we have trivial inequalities between these eigenvalues and some non trivial ones provided by Propositions 2.2 and 2.3.

Table 2.6 summarizes what we know about the eigenvalues in (2.16). In blue the known values, in red the known inequalities. The unknown values should fit in the gray cells.

(σ, τ)	$(\mathcal{T}_h, \mathfrak{dab})$	μ_1		μ_2		μ_3		μ_4
(+, +)	$(\mathcal{T}_h, \mathfrak{dnn})$		<		\leq		\leq	
			\wedge		\wedge		\wedge	\wedge
(+, -)	$(\mathcal{T}_h, \mathfrak{dnd})$	$3 \frac{16\pi^2}{9}$	<	$7 \frac{16\pi^2}{9}$	<	$12 \frac{16\pi^2}{9}$	<	$13 \frac{16\pi^2}{9}$
			\wedge					
(-, +)	$(\mathcal{T}_h, \mathfrak{ddn})$		<		\leq		\leq	
			\wedge		\wedge		\wedge	\wedge
(-, -)	$(\mathcal{T}_h, \mathfrak{ddd})$	$7 \frac{16\pi^2}{9}$	<	$13 \frac{16\pi^2}{9}$	<	$19 \frac{16\pi^2}{9}$	<	$21 \frac{16\pi^2}{9}$

TABLE 2.6. $\mathcal{R}h_e$, Dirichlet boundary condition

From Table 2.6, we conclude that the first Dirichlet eigenvalue for \mathcal{R}_e must be $\mu_1(\mathcal{T}_h, \mathfrak{dnn})$, and that this eigenvalue is simple (which is a well-known fact). The table shows that the second eigenvalue could be $\mu_1(\mathcal{T}_h, \mathfrak{dnd})$ or $\mu_2(\mathcal{T}_h, \mathfrak{dnn})$.

Claim. $\delta_2 < \mu_2(\mathcal{T}_h, \mathfrak{dnn})$. Assume that $\delta_2 = \mu_2(\mathcal{T}_h, \mathfrak{dnn})$, and let u be an eigenfunction associated with δ_2 . Call v its restriction to \mathcal{T}_h . If the nodal set of v contains a closed curve, or a curve from one side to another, except the case of a curve from side 2 to side 3, then u would have too many nodal domains for a second eigenfunction. The only possible case is when the nodal set of v goes from side 2 to side 3, so that u has a closed nodal line. This case is excluded by the “closed nodal line theorem” which holds for any convex set, see [1].

It follows that $\delta_2 = \mu_1(\mathcal{T}_h, \mathfrak{dnd}) = 3 \times \frac{16\pi^2}{9}$. The next smallest eigenvalues are $\mu_2(\mathcal{T}_h, \mathfrak{dnn})$ and $\mu_1(\mathcal{T}_h, \mathfrak{ddn})$, possibly with multiplicity as far as $\mu_2(\mathcal{T}_h, \mathfrak{dnn})$ is concerned.

It follows that

$$(2.17) \quad 0 < \delta_1 < \delta_2 < \delta_3 \leq \delta_4 \leq \dots,$$

and we can a priori not decide whether $\delta_3 = \delta_4$ or not.

Table 2.6 actually provides further information,

$$(2.18) \quad \begin{cases} \dim \mathcal{E}(\delta_1) \cap \mathcal{S}_{+,+} = 1, \\ \mathcal{E}(\delta_1) \cap \mathcal{S}_{\sigma,\tau} = \{0\} \text{ if } (\sigma, \tau) \neq (+, +), \\ \dim \mathcal{E}(\delta_2) \cap \mathcal{S}_{+,-} = 1, \\ \mathcal{E}(\delta_2) \cap \mathcal{S}_{\sigma,\tau} = \{0\} \text{ if } (\sigma, \tau) \neq (+, -). \end{cases}$$

For the reader's convenience, in Table 2.7, we filled the gray cells with the numerical values computed with MATLAB, and inserted the numerical values of the eigenvalues which are explicitly known.

(σ, τ)	$(\mathcal{T}_h, \mathfrak{dab})$	μ_1		μ_2		μ_3		μ_4
(+, +)	$(\mathcal{T}_h, \mathfrak{dnn})$	24.90	<	83.83	\leq	140.50	\leq	169.20
			Λ		Λ		Λ	Λ
(+, -)	$(\mathcal{T}_h, \mathfrak{dn}\mathfrak{d})$	52.64	<	122.82	<	210.55	<	228.10
			Λ					
(-, +)	$(\mathcal{T}_h, \mathfrak{d}\mathfrak{dn})$	71.71	<	169.80	\leq	234.10	\leq	292.70
			Λ		Λ		Λ	Λ
(-, -)	$(\mathcal{T}_h, \mathfrak{d}\mathfrak{d}\mathfrak{d})$	122.82	<	228.10	<	333.37	<	368.47

TABLE 2.7. $\mathcal{R}h_e$, Dirichlet boundary condition

The proof of Proposition 2.12 is complete. \square

Numerical computations show that

$$(2.19) \quad 0 < \delta_1 < \delta_2 < \delta_3 < \delta_4 < \delta_5 = \delta_6 < \delta_7 \cdots$$

with corresponding nodal patterns given by Figure 2.8.

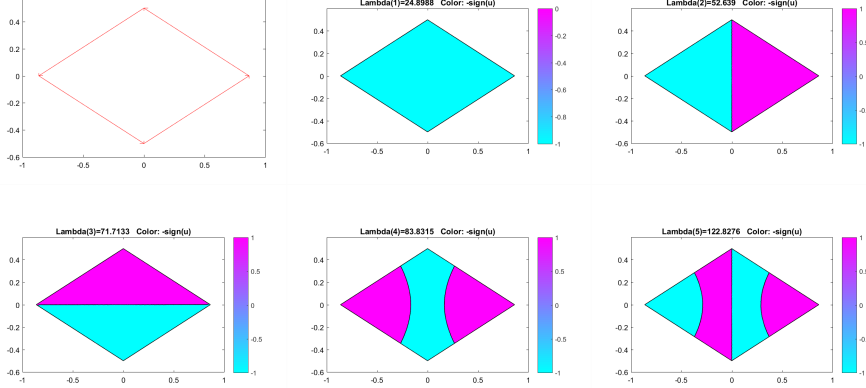


FIGURE 2.8. Rhombus $\mathcal{R}h_e$, Dirichlet boundary condition

Numerical computations also indicate that there are linear combinations in $\mathcal{E}(\delta_2) \oplus \mathcal{E}(\delta_5)$ with 6 nodal domains, thus providing a counterexample to the ECP($\mathcal{R}h_e, \mathfrak{d}$), see Figure 2.9. This counterexample, can also be interpreted as a counterexample to the ECP for the equilateral triangle with mixed boundary conditions, Dirichlet on two sides, and Neumann on the third one.

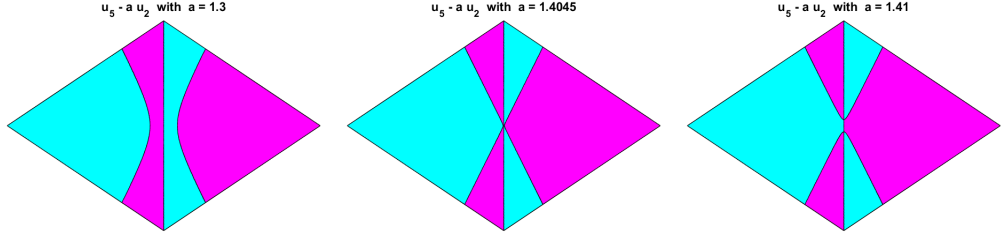


FIGURE 2.9. Counterexample to the ECP($\mathcal{R}h_e$) with Dirichlet boundary condition

Remark 2.13. Looking at the nodal patterns, and in analogy with what we did in the Neumann case, one could think of testing a linear combination in $\mathcal{E}(\delta_1) \oplus \mathcal{E}(\delta_4)$. This gives a linear combination with four nodal domains, which does not contradict Courant's theorem.

3. THE HYPERCUBE

3.1. Preparation. Let $\mathcal{C}_n(\pi) :=]0, \pi[^n$ be the *hypercube* of dimension n , with either the Dirichlet or Neumann boundary condition on $\partial\mathcal{C}_n(\pi)$. A point in $\mathcal{C}_n(\pi)$ is denoted by $x = (x_1, \dots, x_n)$.

A complete set of eigenfunctions of $-\Delta$ for $(\mathcal{C}_n(\pi), \mathfrak{d})$ is given by the functions

$$(3.1) \quad \prod_{j=1}^n \sin(k_j x_j) \text{ with eigenvalue } \sum_{j=1}^n k_j^2, \text{ for } k_j \in \mathbb{N} \setminus \{0\},$$

at the point $x = (x_1, \dots, x_n) \in]0, \pi[^n$.

A complete set of eigenfunctions of $-\Delta$ for $(\mathcal{C}_n(\pi), \mathfrak{n})$ is given by the functions

$$(3.2) \quad \prod_{j=1}^n \cos(k_j x_j) \text{ with eigenvalue } \sum_{j=1}^n k_j^2, \text{ for } k_j \in \mathbb{N}.$$

3.2. Hypercube with Dirichlet boundary condition. In this section, we make use of the classical Chebyshev polynomials $U_k(t)$, $k \in \mathbb{N}$, defined by the relation,

$$\sin((k+1)t) = \sin(t) U_k(\cos(t)),$$

and such that

$$U_0(t) = 1, \quad U_1(t) = 2t, \quad U_2(t) = 4t^2 - 1.$$

The first Dirichlet eigenvalues (as points in the spectrum) are listed in the following table, together with their multiplicities, and eigenfunctions.

TABLE 3.1. First Dirichlet eigenvalues of $\mathcal{C}_n(\pi)$

Eigenv.	Mult.	Eigenfunctions
n	1	$\phi_1(x) := \prod_{j=1}^n \sin(x_j)$
$n + 3$	n	$\phi_1(x) U_1(\cos(x_i))$ for $1 \leq i \leq n$
$n + 6$	$\frac{n(n-1)}{2}$	$\phi_1(x) U_1(\cos(x_i)) U_1(\cos(x_j))$ for $1 \leq i < j \leq n$
$n + 8$	n	$\phi_1(x) U_2(\cos(x_i))$ for $1 \leq i \leq n$

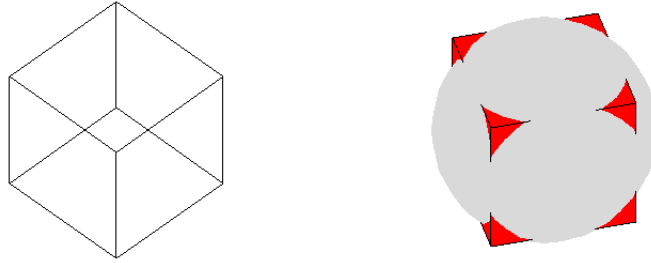


FIGURE 3.1. 3-dimensional cube

For the above eigenvalues, the index defined in Subsection 1.1 is given by,

$$(3.3) \quad \kappa(n+3) = 2, \quad \kappa(n+6) = n+2, \quad \kappa(n+8) = \frac{n(n+1)}{2} + 2.$$

As in [3], in order to study the nodal set of the above eigenfunctions or linear combinations thereof, we use the diffeomorphism

$$(3.4) \quad (x_1, \dots, x_n) \mapsto (\xi_1 = \cos(x_1), \dots, \xi_n = \cos(x_n)),$$

from $]0, \pi[$ onto $-1, 1[$, and factor out the function ϕ_1 which does not vanish in the open hypercube. We consider the function

$$\Psi_a(\xi_1, \dots, \xi_n) = \xi_1^2 + \dots + \xi_n^2 - a$$

which corresponds to a linear combination Φ in $\mathcal{E}(n) \oplus \mathcal{E}(n+8)$. Given some a , $(n-1) < a < n$, this function has $2^n + 1$ nodal domains, see Figure 3.1 in dimension 3. For $n \geq 3$, we have $2^n + 1 > \kappa(n+8)$. The function Φ therefore provides a counterexample to the ECP for the hypercube of dimension at least 3, with Dirichlet boundary condition, thus generalizing [3, Section 2].

Proposition 3.1. *For $n \geq 3$, the hypercube of dimension n , with Dirichlet boundary condition, provides a counterexample to the ECP.*

Remark. An interesting feature of this example is that we get counterexamples to the ECP for linear combinations which involve eigenvalues with high energy while the examples in [3] only involve eigenvalues with low energy. This is also in contrast with the fact that, in dimension 3, Courant's nodal domain theorem is sharp only for δ_1 and δ_2 , [5].

3.3. Hypercube with Neumann boundary condition. In this section, we make use of the classical Chebyshev polynomials $T_k(t)$, $k \in \mathbb{N}$, defined by the relation,

$$\cos(kt) = \cos(t) T_k(\cos(t)),$$

and such that

$$T_0(t) = 1, \quad T_1(t) = t, \quad T_2(t) = 2t^2 - 1.$$

The first Neumann eigenvalues (as points in the spectrum) are listed in the following table, together with their multiplicities, and eigenfunctions.

TABLE 3.2. First Neumann eigenvalues of $\mathcal{C}_n(\pi)$

Eigenv.	Mult.	Eigenfunctions
0	1	$\psi_1(x) := 1$
1	n	$T_1(\cos(x_i))$ for $1 \leq i \leq n$
2	$\frac{n(n-1)}{2}$	$T_1(\cos(x_i)) T_1(\cos(x_j))$ for $1 \leq i < j \leq n$
3	$\frac{n(n-1)(n-2)}{6}$	$T_2(\cos(x_i))$ for $1 \leq i \leq n$
4	$n + \binom{n}{4}$	$T_2(\cos(x_i))$ for $1 \leq i \leq n$ and ...

For the above eigenvalues, the index defined in Subsection 1.1 is given by,

$$(3.5) \quad \kappa(2) = n + 2, \quad \kappa(3) = \frac{n(n+1)}{2} + 2, \quad \kappa(4) = \frac{n(n^2+5)}{6} + 2.$$

As in [3], in order to study the nodal set of the above eigenfunctions or linear combinations thereof, we use the diffeomorphism

$$(3.6) \quad (x_1, \dots, x_n) \mapsto (\xi_1 = \cos(x_1), \dots, \xi_n = \cos(x_n)),$$

from $]0, \pi[$ onto $] -1, 1[$, and factor out the function ϕ_1 which does not vanish in the open hypercube. We consider the function

$$\Psi_a(\xi_1, \dots, \xi_n) = \xi_1^2 + \dots + \xi_n^2 - a,$$

which corresponds to a linear combination Φ in $\mathcal{E}(0) \oplus \mathcal{E}(4)$. Given some a , $(n-1) < a < n$, this function has $2^n + 1$ nodal domains. For $n \geq 4$, we have $2^n + 1 > \kappa(4)$. The function Φ therefore provides a counterexample

to the ECP for the hypercube of dimension at least 4, with Neumann boundary condition, thus providing a new counterexample.

Proposition 3.2. *For $n \geq 4$, the hypercube of dimension n , with Neumann boundary condition, provides a counterexample to the ECP.*

Remark. An interesting feature of this example is that we get counterexamples to the ECP for linear combinations which involve eigenvalues with high energy while the examples in [3] only involve eigenvalues with low energy.

REFERENCES

- [1] G. Alessandrini. Nodal lines of eigenfunctions of the fixed membrane problem in general convex domains, *Comment. Math. Helvetici* 69 (1994), 142–154. [13](#)
- [2] P. Bérard and B. Helffer. Courant-sharp eigenvalues for the equilateral torus, and for the equilateral triangle. *Letters in Math. Physics* 106 (2016), 1729–1789. [6](#)
- [3] P. Bérard and B. Helffer. On Courant’s nodal domain property for linear combinations of eigenfunctions. *arXiv:1705.03731*. [2](#), [6](#), [10](#), [16](#), [17](#), [18](#)
- [4] R. Courant and D. Hilbert. *Methods of mathematical physics. Vol. 1.* First English edition. Interscience, New York 1953. [2](#)
- [5] B. Helffer and R. Kiwan. Dirichlet eigenfunctions on the cube, sharpening the Courant nodal inequality. *arXiv: 1506.05733*. [17](#)
- [6] H. Herrmann. *Beiträge zur Theorie der Eigenwerte und Eigenfunktionen.* Göttinger Dissertation defended May 20, 1931. Teubner 1932. [2](#)
- [7] V. Lotoreichik and J. Rohleder. Eigenvalue inequalities for the Laplacian with mixed boundary conditions. *J. Differential Equations* 263 (2017) 491–508. [5](#), [8](#)
- [8] B. Siudeja. On mixed Dirichlet-Neumann eigenvalues of triangles. *Proc. Amer. Math. Soc.* 144 (2016) 2479–2493. [5](#), [8](#), [10](#)

PB: INSTITUT FOURIER, UNIVERSITÉ GRENOBLE ALPES AND CNRS, B.P.74, F38402 SAINT MARTIN D’HÈRES CEDEX, FRANCE.

E-mail address: pierrehberard@gmail.com

BH: LABORATOIRE JEAN LERAY, UNIVERSITÉ DE NANTES AND CNRS, F44322 NANTES CEDEX, FRANCE.

E-mail address: Bernard.Helffer@univ-nantes.fr